Stack Concepts for High Temperature Polymer Electrolyte Membrane Fuel Cells

Holger Janßen, Jen Supra, and Werner Lehnert

20.1 Introduction

Stationary and mobile applications are attractive applications for high temperature polymer electrolyte membrane fuel cells (HT-PEMFC). Examples for stationary applications are electricity and heat generation for households or uninterruptible power supply (UPS) systems. In the case of mobile applications the on board power supply with auxiliary power units (APUs) and backup power for the recreation area are most promising. In comparison to the low temperature PEMFC (operated at 60–80 °C) the operating temperature of a HT-PEMFC, which is between 120 and 200 °C, allows a more effective co-generation of power and heat. The higher temperature also leads to an improved tolerance to fuel impurities and a simpler system design [1]. Therefore applications where hydrogen is generated with reformer systems are ideally suited for a HT-PEMFC due to the increased CO tolerance [1, 2]. The majority of these demands have electric power requirements between some hundred Watt and the low kW range.

In order to meet the power demands for those applications HT-PEM single cells must be stacked. In comparison to single cells with usually small active MEA areas less than 100 cm^2 a HT-PEMFC stack challenges further tasks, for example, the gas distribution inside each cell of the stack. Another major topic where single cell behavior cannot be used to predict stack behavior is the heat management. Even for applications in the power range of several 100 W up to the kW range stack cooling is a major design criterion for the stack development. HT-PEMFC stacks perform advantageously when they are used in reformate operation. However, this greatly affects the heat management of the stack. In order to develop a suitable heat management system and with this an appropriate stack design, knowledge of the thermal behavior is required.

20.2 Basic Stack Concepts

The difference between HT-PEM single cells and stacks is usually the increasing cell number with more than one cell and the size of the active MEA area. These are the main parameters for a power related sizing of the stack. In a first step we consider a single cell to evaluate the influence of the active cell area on the electric power. As a basis for the calculations the experimentally determined standardized polarization curve for reformate operation, shown in Fig. 20.1, was
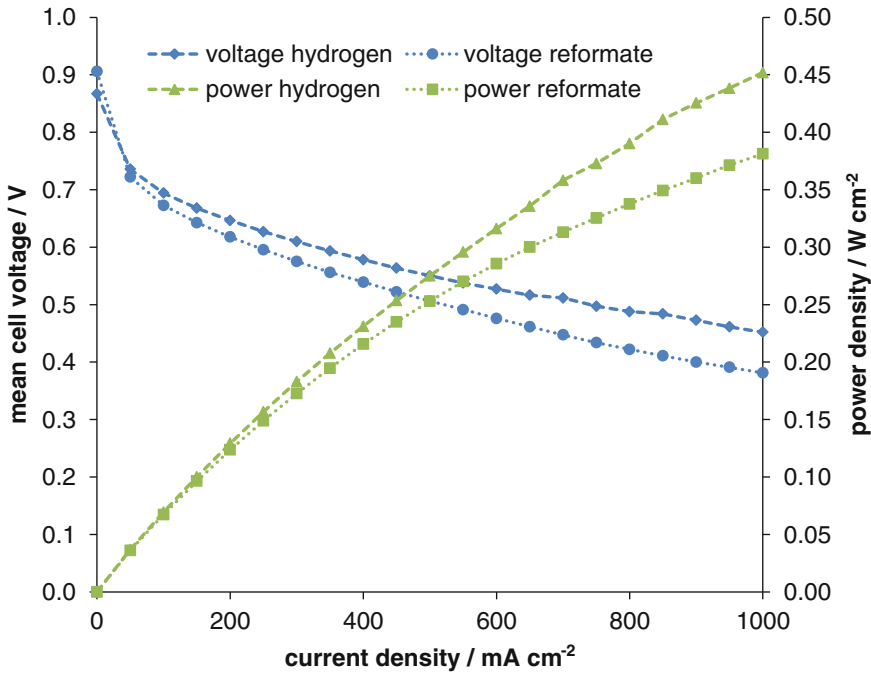
H. Janßen (✉) • J. Supra
Forschungszentrum Jülich GmbH, Jülich, Germany
e-mail: h.janssen@fz-juelich.de

W. Lehnert
Institute of Energy and Climate Research,
Electrochemical Process Engineering (IEK-3),
Forschungszentrum Jülich GmbH, Jülich, Germany

Fig. 20.1 Mean cell voltage and power density for a HT-PEMFC stack operated with hydrogen/air and synthetic reformate/air. Operating conditions according to Table 20.1, MEA used: BASF Celtec® P-1000 [3]

Table 20.1 Reference conditions

Parameter	Value
Number of cells	10
Active cell area	200 cm^2
Anode stoichiometry λ_{an}	2
Cathode stoichiometry λ_{ca}	2
Gas inlet temperature	160 °C
Liquid coolant inlet temperature	160 °C
Reformate composition	42 vol% H$_2$, 1 vol% CO, and 57 vol% N$_2$

used. The results for different current densities at the reference conditions (except number of cells and active cell area), given in Table 20.1, are shown in Fig. 20.2.

From Fig. 20.2 it can be seen that there is a linear increase of the produced electric power with increasing active cell area under the assumption that scaling up of the active area does not influence the cell behavior. For a current density of 450 mA cm^{-2} at reformate operation the produced electric power increases from 2.35 W at 10 cm^2 active cell area to 235 W at 1000 cm^2. For the designated applications in the power range of some hundred watts or even

higher an active cell area of more than 1000 cm^2 is necessary. A setup with only one single cell is extremely challenging because of the very high demands on the gas distribution, active heat dissipation and manufacturing accuracy due to sealing requirements and MEA compression. Additionally the low voltage of a single cell setup in the range of 0.5–0.6 V is not useful for most applications. A step-up converter has to be introduced. For these reasons it is advisable to reduce the active cell area and use more cells. Cell areas between 100 and 350 cm^2 are ideally suited to fulfill the requirements for the targeted power range between some hundred Watt and
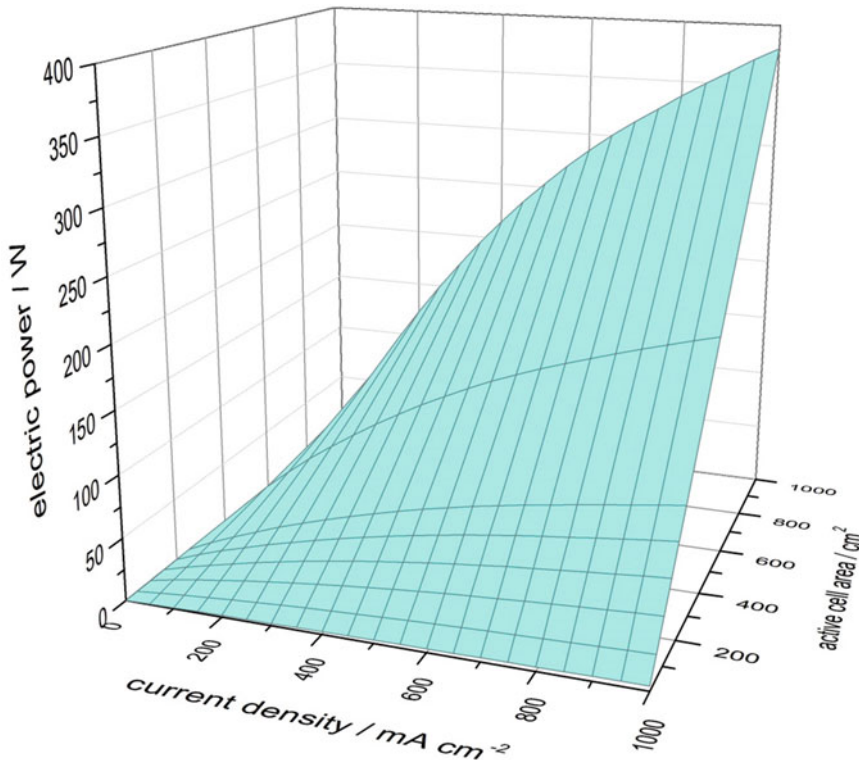
Fig. 20.2 Influence of the active cell area on the produced electric power for a single cell at reformate operation

some kilo Watt. For this reason, the following considerations will be carried out on HT-PEMFC stack concepts having a cell area of 200 cm^2. The influence of the cell number on the produced electric power for such a stack is shown in Fig. 20.3. Here it is assumed that each cell performs on the same level.

Corresponding to the curve shape in Fig. 20.2 the generated electric power increases linearly with increasing number of cells. For a common current density of 450 mA cm^{-2} the produced electric power rises from 47 W for 1 cell up to 4700 W for 100 cells.

It can be concluded for a reformate stack operation that active cell areas between 100 and 350 cm^2 and cell numbers between 10 and 100 are technically feasible and suitable for the most envisaged applications which was also demonstrated by different groups [4, 5]. The scalability of fuel cell stacks in terms of active cell area and number of cells and also the modularity of a fuel cell system give the stack and systems designer some degrees of freedom.

Possible application oriented target parameters for the stack development are, e.g., space restrictions or nominal voltages. Especially a high voltage transfer ratio from stack to systems voltage possibly affects the systems efficiency negatively due to the increased losses of the converter.

For the development of HT-PEMFC stacks it is essential to determine detailed knowledge about the thermal behavior. Calculations and experimental investigations are key aspects of the following sections.

20.3   Energy Balance for a HT-PEMFC Stack

For a first approach the energy balance equation has to be solved for a simplified stack model. The stack is assumed to be ideally insulated and the stack is in a steady state operation. The energy balance control volume is given in Fig. 20.4.
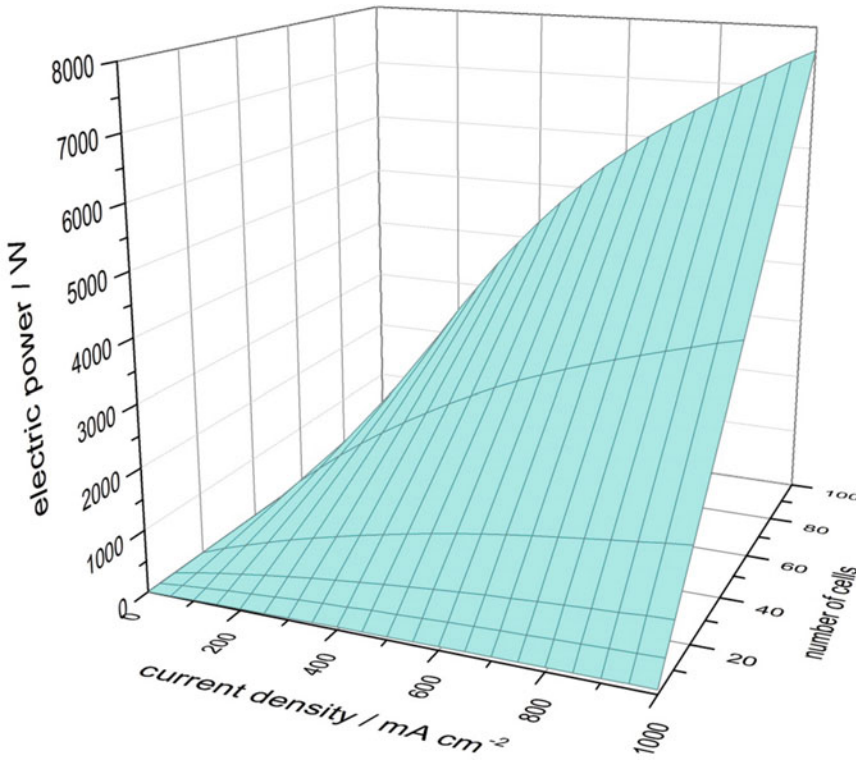
Fig. 20.3 Influence of the number of cells on the produced electric power for a HT-PEMFC stack with 200 cm² active cell area at reformate operation
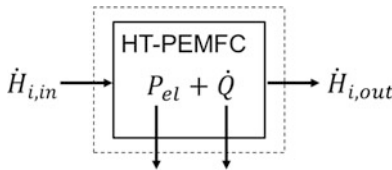

Fig. 20.4 Energy balance control volume

With this simplified model the percentage of heat to be removed ($\dot{Q}$) by the stack cooling system can be identified by solving 20.1, where $\dot{H}_{i,\,in}$ is the enthalpy of component i at the inlet of the control volume, $\dot{H}_{i,\,out}$ is the enthalpy of component i at the outlet, $\dot{Q}$ is the heat to be removed by the cooling medium, and P_{el} is the produced electrical power output of the stack.

$$\sum \dot{H}_{i,\,in} = P_{el} + \sum \dot{H}_{i,\,out} + \dot{Q} \qquad (20.1)$$

The electrical power output depends on the operating conditions and the gases used for stack operation. Due to the lower cell efficiency in reformate operation compared to hydrogen operation at the same stack power a distinction between pure hydrogen operation and the operation with different reformate compositions has to be made [6]. In the following, dry reformate gas based on a diesel reforming process is taken into account. This reformate contains 42 vol% H_2, 1 vol% CO, and other gases (mostly CO_2) which are replaced here by N_2 (57 vol%) because of their inert behavior in HT-PEMFC operation [7, 8]. All anode side gases with the exception of hydrogen are considered as inert gases in the energy balance. With this assumption 20.1 can be specified for hydrogen/air operation (20.2) and reformate/air operation (20.3).

$$\dot{Q} = -P_{el} + \dot{H}_{air,\,in} + \dot{H}_{H_2,\,in} - \dot{H}_{air,\,out}$$
$$- \dot{H}_{H_2,\,out} - \dot{H}_{H_2O,\,out} \qquad (20.2)$$

Table 20.2 Enthalpy and mass flow equations

Incoming enthalpy flows	Outgoing enthalpy flows
$\dot{H}_{\text{air, in}} = \dot{m}_{\text{air, in}} \cdot c_{p,\text{ air}} \cdot \vartheta_{\text{in}}$	$\dot{H}_{\text{air, out}} = \left(\dot{m}_{\text{O}_2,\text{ out}} \cdot c_{p,\text{ O}_2} + \dot{m}_{\text{N}_2,\text{ out}} \cdot c_{p,\text{ N}_2} \right) \cdot \vartheta_{\text{out}}$
$\dot{H}_{\text{H}_2,\text{ in}} = \dot{m}_{\text{H}_2,\text{ in}} \cdot \left(c_{p,\text{ H}_2} \cdot \vartheta_{\text{in}} + h^0_{\text{HHV}} \right)$	$\dot{H}_{\text{H}_2,\text{ out}} = \dot{m}_{\text{H}_2,\text{ out}} \cdot \left(c_{p,\text{ H}_2} \cdot \vartheta_{\text{out}} + h^0_{\text{HHV}} \right)$
$\dot{H}_{ig,\text{ in}} = \dot{m}_{ig,\text{ in}} \cdot c_{p,\,ig} \cdot \vartheta_{\text{in}}$	$\dot{H}_{ig,\text{ out}} = \dot{m}_{ig,\text{ out}} \cdot c_{p,\text{ out}} \cdot \vartheta_{\text{out}}$
	$\dot{H}_{\text{H}_2\text{O, gen}} = \dot{m}_{\text{H}_2\text{O, gen}} \cdot \left(c_{p,\text{ H}_2\text{O, gen}} \cdot \vartheta_{\text{out}} + h^0_{fg} \right)$
Incoming mass flows	**Outgoing mass flows**
$\dot{m}_{\text{air, in}} = \frac{\lambda_{\text{O}_2}}{\chi_{\text{O}_2}} \cdot \frac{M_{\text{air}}}{4F} \cdot I \cdot n_{\text{cell}}$	$\dot{m}_{\text{O}_2,\text{ out}} = \left(\lambda_{\text{O}_2} - 1 \right) \cdot \frac{M_{\text{O}_2}}{4F} \cdot I \cdot n_{\text{cell}}$
	$\dot{m}_{\text{N}_2,\text{ out}} = \frac{\left(1 - \chi_{\text{O}_2} \right)}{\chi_{\text{O}_2}} \cdot \frac{M_{\text{N}_2}}{4F} \cdot I \cdot n_{\text{cell}}$
$\dot{m}_{\text{H}_2,\text{ in}} = \lambda_{\text{H}_2} \cdot \frac{M_{\text{H}_2}}{2F} \cdot I \cdot n_{\text{cell}}$	$\dot{m}_{\text{H}_2,\text{ out}} = \left(\lambda_{\text{H}_2} - 1 \right) \cdot \frac{M_{\text{H}_2}}{2F} \cdot I \cdot n_{\text{cell}}$
$\dot{m}_{ig,\text{ in}} = \frac{1 - \chi_{\text{H}_2}}{\chi_{\text{H}_2}} \cdot \frac{M_{ig}}{2F} \cdot I \cdot n_{\text{cell}}$	$\dot{m}_{ig,\text{ out}} = \dot{m}_{ig,\text{ in}} = \frac{1 - \chi_{\text{H}_2}}{\chi_{\text{H}_2}} \cdot \frac{M_{ig}}{2F} \cdot I \cdot n_{\text{cell}}$
	$\dot{m}_{\text{H}_2\text{O, gen}} = \frac{M_{\text{H}_2\text{O}}}{2F} \cdot I \cdot n_{\text{cell}}$

$\dot{H}_i$: Enthalpy flow of component i, W
$\dot{m}_i$: Mass flow of component i, kg s^{-1}
$c_{p,i}$: Specific heat capacity of component i, J kg^{-1} K^{-1}
ϑ: Temperature difference to the reference temperature (0 °C), K
h^0_{HHV}: Higher heating value of hydrogen at reference temperature, J kg^{-1}
h^0_{fg}: Enthalpy of condensation for water at reference temperature, J kg^{-1}
λ_i: Stoichiometric factor for component i, –
χ_i: Mass fraction of component i, –
M_i: Molar mass of component i, kg mole^{-1}
I: Electric current, A
$F = 96{,}485$ A s mol^{-1}: Faraday constant
n_{cell}: Number of cells, –

$$\dot{Q} = -P_{\text{el}} + \dot{H}_{\text{air, in}} + \dot{H}_{\text{H}_2,\text{ in}} + \dot{H}_{ig,\text{ in}}$$
$$- \dot{H}_{\text{air, out}} - \dot{H}_{\text{H}_2,\text{ out}} - \dot{H}_{\text{H}_2\text{O, out}}$$
$$- \dot{H}_{ig,\text{ out}} \tag{20.3}$$

The required enthalpy for the calculation can be determined using the equations shown in Table 20.2, for tabulated values (e.g., [9]) and the mass flow rates calculated from Faraday's law. The reference temperature for the energy balance is set to 0 °C.

To determine the heat flux to be dissipated, the value for the generated electric power is still missing. One possible way is to determine the electric power experimentally. For a HT-PEMFC stack operation with hydrogen/air, respectively, reformate/air at reference conditions defined in Table 20.1 the measured values are shown in Fig. 20.1.

From Fig. 20.1 it can be seen that for all current densities the voltage efficiency for pure hydrogen operation is higher than for the synthetic reformate operation due to the lower hydrogen concentration and the CO content in the reformate. The difference in the average power density in the whole current density range shown in Fig. 20.2 is about 10 %. Using these experimentally determined values for P_{el}, the energy balance equation for pure hydrogen/air and reformate/air operation can be solved. The results are shown in Fig. 20.5.

It can be seen that a waste heat flow of 0.86 W cm^{-2} at 1000 mA cm^{-2} in reformate operation has to be removed from the stack. For an ideally insulated HT-PEMFC stack this heat flux must be dissipated exclusively by the thermal management system to maintain a steady operating temperature. Due to the higher amount of heat to be dissipated at a given current density (in average 6 %) in comparison to the pure hydrogen operation the reformate operation is the design reference for the thermal management system and with this as well for the stack concept.
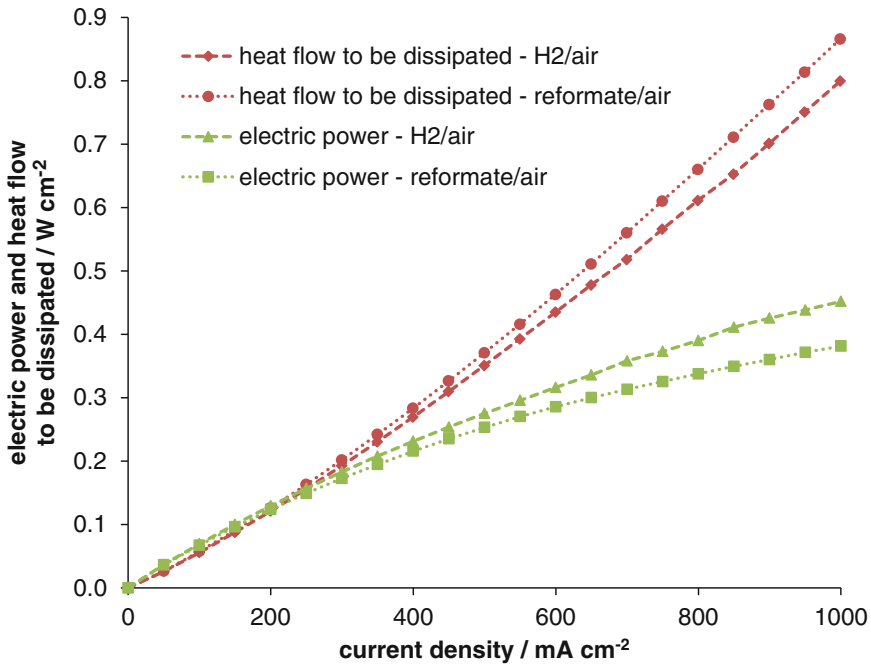
Fig. 20.5 Results of the energy balance on the basis of the experimentally determined electric power (*green curves*). Calculated heat flow (*red curves*) for hydrogen/air and reformate/air operation

20.4 Thermal Management of a HT-PEMFC Stack

The thermal management has a high impact on the HT-PEMFC stack concept when changing from single cells to stacks. Therefore this sub-chapter focuses on basic thermal management concepts for HT-PEMFC stacks. First, principal methods of heat removal from the heat generating MEA are explained, focusing on the possible heat transfer media. Both directly affect the stack concept. The thermal management system needs to provide cooling during operation and heat up on temperatures above 100 °C at the start-up process when the stack will be operated with hydrogen or to a temperature of 160 °C when reformate gas will be used. During operation local temperatures below 100 °C lead to condensation of product water. Phosphoric acid will be lost by leaching and the protonic conductivity will be reduced. When operated with reformate the higher temperature is necessary due to the poisoning effect of CO at low temperatures.

For a HT-PEMFC stack the generated heat must be taken out of the stack according to the energy balance (see Sect. 20.3). Figure 20.6 shows different methods to transport, transfer, and remove the heat.

Basically a distinction between internal and external cooling is made. For internal cooling the heat generated in the MEAs will be carried out of the stack by means of a liquid or gaseous heat transfer medium flowing through the fuel cell stack. A special case for internal cooling is the adaption of the air flow rate on the cathode side to a value which is sufficient for the heat removal. The heat transport between the MEAs and the internal flow structures of the heat transfer medium takes place due to heat conduction through the solid stack materials driven by the temperature difference. For the external cooling the heat transport takes place by means of heat conduction via the stack materials to the surface of the stack, where the heat transfer takes place. This can happen either by means of forced convection to a heat transfer fluid flowing at the outside or by means of free convection and radiation to the surrounding environment. The
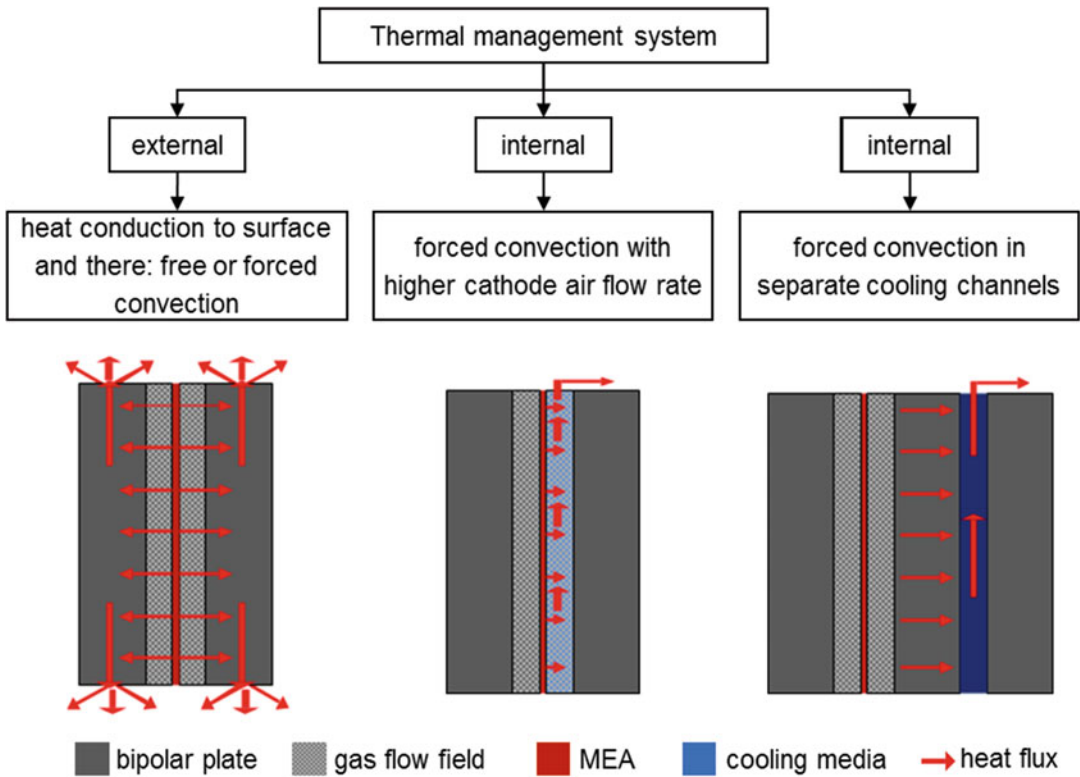
Fig. 20.6 Different methods for heat removal from HT-PEMFC stacks

heat discharge by natural convection and radiation at the surface of the fuel cell stack is equivalent to a purely passive cooling.

These three basic thermal management concepts influence the stack design in various ways. In the following, some possible designs and their influence on the operating behavior of the stack are considered. For all considerations stacks with an active area of 200 cm^2 are used as previously defined.

20.4.1 Passive Cooling of HT-PEMFC Stacks

In this section stack concepts with an external thermal management will be discussed. If the heat transfer at the surface of the stack takes place only by radiation and free convection no additional power consumption for the cooling is necessary. In addition, it requires no further

components for the heat conduction if the already used stack materials have proper heat conductivity. The amount of heat to be dissipated strongly depends on the surface area and the temperature difference between the HT-PEMFC stack surface and the surrounding which is mostly ambient air. Due to the fixed operating temperature of around 160 °C, the more or less constant ambient temperature and under the assumption of sufficient thermal conductivity of the stack material only the stack surface can be modified to have an influence on the heat dissipation. This directly leads to changes in the HT-PEMFC stack design. Therefore the influence of the surface area on the dissipated heat must be calculated in order to determine whether this thermal management concept provides sufficient heat dissipation or not. Exemplary this is done in the following for a stack with an active cell area of 200 cm^2. The stack design is inspired by the stack described in Table 20.4 except that the internal cooling
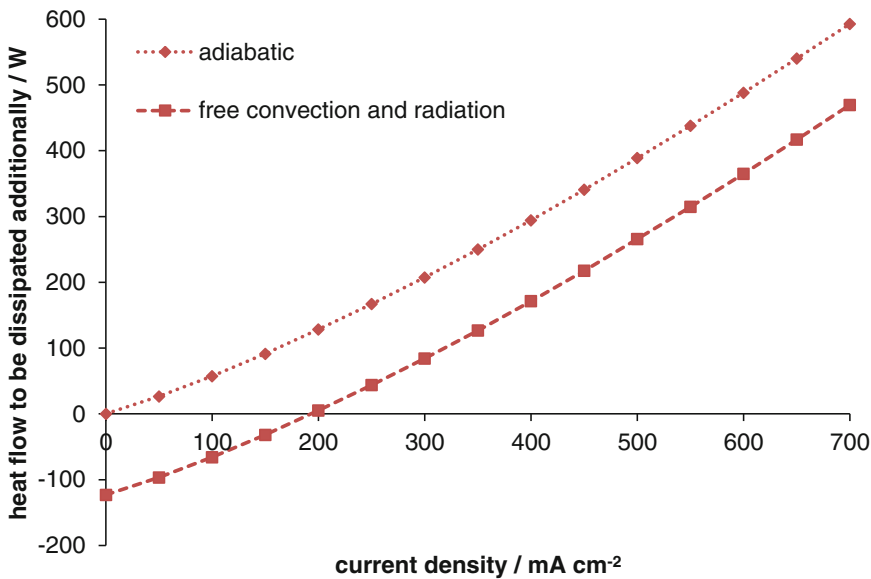
Fig. 20.7 Energy balance based calculation of the heat flow to be dissipated by an additional cooling system, five cells, $A_{\text{act}} = 200 \text{ cm}^2$, $t_{\text{Stack}} = 160\,^{\circ}\text{C}$, $t_{\text{amb}} = 20\,^{\circ}\text{C}$

structures are omitted. Considering that the heat dissipation takes place at the surface only by free convection and radiation the energy balance equation has been solved for an exemplary stack with five cells and an active cell area of 200 cm^2. For the calculations the stack temperature and with this the surface temperature is fixed at $160\,^{\circ}\text{C}$ and the ambient temperature is fixed to $20\,^{\circ}\text{C}$. The results are shown in Fig. 20.7 and compared with a thermal ideally insulated stack (adiabatic boundary conditions).

In comparison to the adiabatic stack, of course less heat needs to be removed additionally for the not insulated stack. However, as Fig. 20.7 shows only one operating point at a current density of 200 mA cm^{-2} exists, where no additional cooling besides the passive surface cooling is necessary. At this operating point a steady stack operation would be possible at the chosen temperature of $160\,^{\circ}\text{C}$. For a stack operation at higher current densities additional cooling is necessary, or the temperature will increase. For lower current densities a heating must be provided even at steady-state operation. In order to accomplish increased heat dissipation, the surface area can be increased by additional parts (like, e.g., fins). Another possibility to enlarge the stack surface

for the heat transfer is to change the aspect ratio of the MEA, respectively, bipolar plate edges at a constant active cell area. Calculations show that the effect of the ratio change is small. If the ratio of the active cell area is changed from 141×141 to $50 \times 400 \text{ mm}^2$ only 4 % more heat will be dissipated over the enlarged surface [10]. Another disadvantage of this cooling system is the dependence on the number of cells. For most applications an increased number of cells are required. With this, the influence of the surface cooling decreases.

Figure 20.8 shows that the influence of surface cooling decreases with increasing number of cells. The current density where steady-state stack operation at $160\,^{\circ}\text{C}$ is possible decreases with increasing number of cells. The reason is the decreasing influence of the end plates surface and the associated lower surface to active cell area ratio with high cell numbers. As a result of the increasing heat production with increasing number of cells, small changes in the current density have a high impact on the heat to be dissipated additionally by active cooling due to the increasing slope of the curve. The current density range where an active heat supply is necessary is reduced from 200 mA cm^{-2} down to 25 mA cm^{-2}
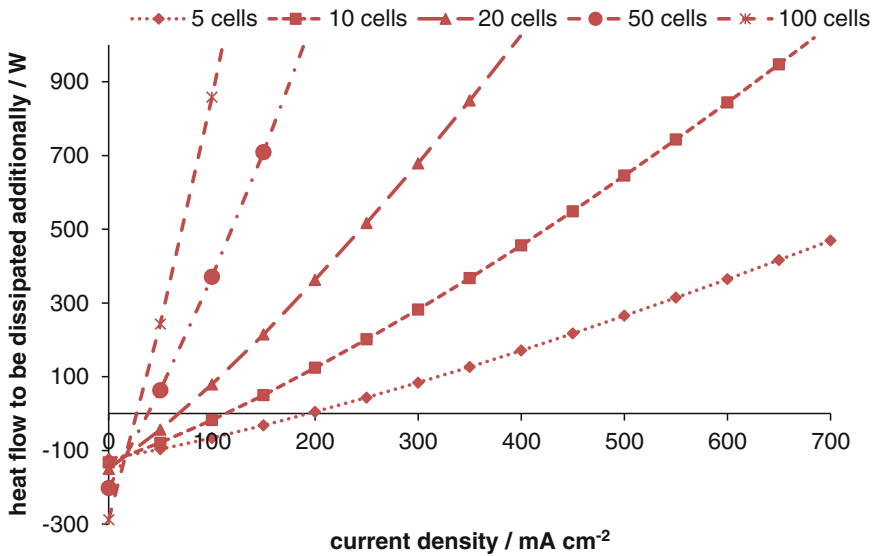
Fig. 20.8 Influence of the number of cells on the heat flow to be dissipated, $A_{act} = 200$ cm^2, $t_{Stack} = 160$ °C, $t_{amb} = 20$ °C

by increasing the number of cells from 5 to 100. This also means that a purely passive cooled stack with 100 cells can only be operated at the fixed boundary conditions setting the current density to a value of 25 mA cm^{-2}. At this operating point the generated electric power is only 360 W (18 mW cm^{-2}). Thus, a high number of cells reduce the impact of the external surface cooling on the total cooling effort.

It can be concluded that a stack concept with pure passive cooling is not advisable because the stack temperature varies strongly with the stack power and as a result the specified temperature range may be exceeded. Dependent on the stack power (full load, partial load) during normal operation additional cooling or heating is required. Therefore an active thermal management system is mandatory.

20.4.2 Active Cooling of HT-PEMFC Stacks

One possibility for an internal thermal management concept is the cooling with increased and adapted cathode air flow rate. This influences the HT-PEMFC stack design only slightly. Only the cathode flow field structure needs to be adjusted to the higher air flow rate to restrict the parasitic power consumption by the fan or compressor. Previously, some HT-PEMFC stacks have been studied and developed according to this concept. For all stack concepts the power range is limited to a maximum of around 1 kW$_{el}$ and the maximum active cell area is restricted to 50 cm^2 [11–15]. Moreover, experiences from the low temperature PEMFC show that this type of stack cooling with a power generation of more than 5 kW$_{el}$ is insufficient or not advantageous [16, 17]. Nevertheless, for the here examined stack concept with an active area of 200 cm^2 and exemplary ten cells, the prerequisites for a potential cathode air cooling will be calculated. Further boundary conditions are reformate operation, a cathode air inlet temperature of 25 °C and an outlet temperature of 160 °C. The heat to be dissipated is calculated using the energy balance equation. The required cathode air flow for steady state stack operation is shown in Table 20.3.

As Table 20.3 shows, the necessary cathode stoichiometry is between 11 and 18 for a temperature difference of 135 K between incoming and exiting air. Using a meander type flow field with

Table 20.3 Required cathode air flow rates for appropriate cooling

Current density/ mA cm^{-2}	Heat flow to be dissipated/W	Required cathode air flow rate/m^3 h^{-1}	Stoichiometry
50	53	1.4	11
100	115	2.8	12
150	182	4.6	13
200	257	6.7	14
250	334	8.5	14
300	415	10.6	15
350	500	13.1	15
400	589	15.3	16
450	681	17.7	16
500	778	20.2	17
550	876	22.7	17
600	976	25.5	17
650	1080	28.0	18
700	1185	30.9	18

Table 20.4 Parameters of the HT-PEMFC stack concept with internal cooling

Stack component	Specification
MEA type	BASF Celtec® P-1000 [3]
Active cell area	200 cm^2 (110 mm × 182 mm), reference, cf. Table 20.1
Number of cells	10, reference, cf. Table 20.1
Gaseous cooling fluid	Ambient air
Liquid cooling fluid	FRAGOLTHERM® S-15-A, polyglycol based [20]
Cooling flow field	45 straight rectangular channels (1.5 mm × 2 mm)
Bipolar plate material	Composite of graphite and phenolic resin, Eisenhuth BBP 4 [21]
Anode side flow field	10 parallel meanders; channel width/depth: 1 mm/1 mm, land width: 1 mm
Cathode side flow field	Same design as anode side flow field
End plates	Aluminum
Thermal insulation	>20 mm silicon foam

parameters given in Table 20.4 results in a high cathode side pressure drop at elevated air stoichiometry. A Computational Fluid Dynamics (CFD) simulation of the structure showed a pressure drop of 149.8 Pa at a comparatively low air stoichiometry of 2 [18]. Increasing the stoichiometry to values feasible for the heat removal leads to parasitic power consumptions of more than 10 % of the produced electric power even if the flow field structure would be changed from meander type to straight channels [10]. Another drawback is the heat integration in the system or application using air as the heat transfer medium. Compared to liquid cooling media the specific heat capacity and the heat transfer coefficient are significantly lower. Therefore this concept is

suitable to fulfill the thermal management of stacks in the kW range. Nevertheless, the simple stack construction and the low space and weight requirements provide an attractive way of cooling for applications with low power consumption.

Another possibility for an active thermal management concept is to use cooling channels which are separated from the anode and cathode side gas channels.

Due to separate cooling flow fields which prevent a mixture of the cooling media and reactant gases and also a contact with the MEA, different possible cooling media can be used. Generally the cooling medium should not be electrically conductive, absorb and release heat
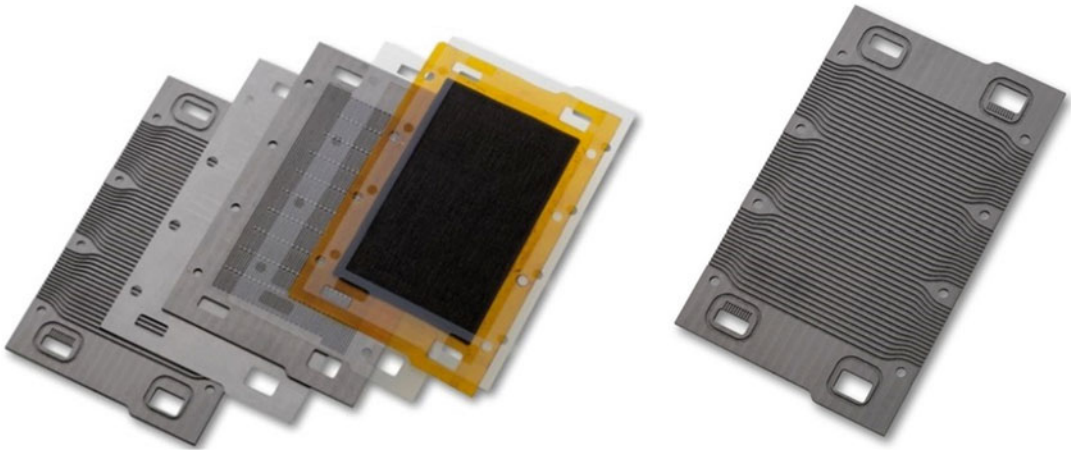
Fig. 20.9 Repeating unit of the basic stack setup (*left*); coolant flow field on the rear of the cathode side bipolar plate half-shell (*right*)

in the temperature range of the HT-PEMFC, have a low viscosity to restrict the pressure drop in the cooling circuit, and should not be harmful to the environment. In general, three different cooling media classes can be defined:

- Fluids which are gaseous in the whole temperature operating range of the HT-PEMFC. Here air is the preferred medium.
- Fluids which stay liquid in the whole temperature operating range. Here a broad range of different products exist. The majority is based on mineral oil or polyglycol. Necessarily the evaporation temperature is above 200 °C. For the further discussion these products are collectively referred to oil.
- Fluids with phase changes during cooling and heat-up. Here water is the best known representative.

For the internal thermal management concept with forced convection in separate cooling channels, the bipolar plates are split into two half-shells. The cooling channels can either be integrated into the bipolar plate material on the back side of one of the half-shells or within separate cooling cells. Both methods allow the usage of different heat transfer media.

In the following we will experimentally analyze and compare stack concepts on the basis of

active cooling with air and oil. To eliminate influences coming from different test setups, cell sizes, and stacks the investigations were performed using the same basic stack components. Figure 20.9 shows the elements of the repeating unit. It consists of two bipolar plate half-shells connected with an electrically conductive flat gasket from expanded graphite (Sigraflex®) and a MEA with two non-conductive flat gaskets from perfluoroalkoxy polymer (PFA).

The bipolar plates comprise flow field structures with a total area of 200 cm^2. As for the MEA the dimensions are 110 mm × 182 mm. The gas flow fields on the anode and on the cathode side are equal due to similar flow rates of air and reformate (diesel based) at stack operation. The flow field structures consist of ten parallel meanders. On the back of the cathode side bipolar plate half-shell, straight channels for the heat transfer media flow are integrated. Sealing is achieved if the stack is clamped using tie rods.

From these basic components stacks were assembled as shown in Fig. 20.10. The supply and removal of the liquid heat transfer media and the distribution on every cell is provided by externally mounted manifolds. The heat transfer fluids flow from the top downwards through the straight channel structure on the back of the cathode side half-shell.
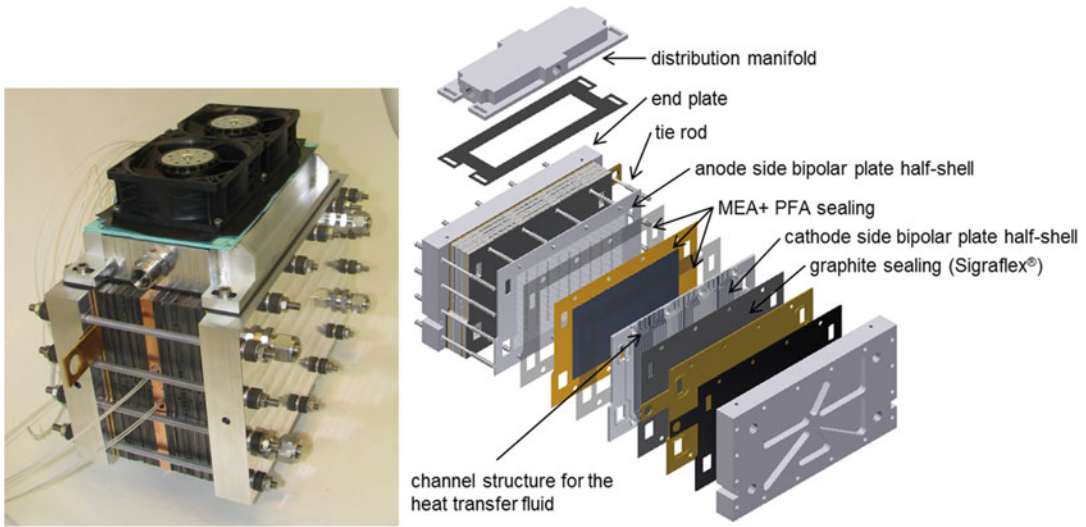
Fig. 20.10 Basic HT-PEMFC stack concepts with internal air cooling (*left*) and internal liquid cooling (*right*) [19]

Table 20.5 Experimental boundary conditions

Stack component	Design
Anode gas	Synthetic reformate, composition: reference, cf. Table 20.1
Cathode gas	Air
Stoichiometry	$\lambda_{an/ca} = 2/2$, reference, cf. Table 20.1
Gas inlet temperature	160 °C, reference, cf. Table 20.1
Inlet temperature cooling air	Ambient temperature, 20–25 °C
Inlet temperature liquid coolant	160 °C, reference, cf. Table 20.1
Cooling air mass flow	2.2 kg min^{-1} in total
Liquid coolant mass flow	4 kg min^{-1} in total

For the stack setup with air cooling (Fig. 20.10, left) two axial blowers are mounted on top of the distributor manifold. Heat-up of the stack is achieved by heating cartridges integrated in the center plate of the stack. In the case of the stack setup with liquid cooling (Fig. 20.10, right) two external manifolds (top and bottom (not shown in Fig. 20.10) of the stack) are necessary to realize a closed oil loop. Heat-up and cooling of the oil is done by heat exchangers integrated into the test station. In Table 20.4 the specification of the stack setups are summarized.

The shown stack concept is used to determine the temperature distribution across the active cell area. Further experimental boundary conditions are listed in Table 20.5.

For the air cooled stack setup the results of the temperature distribution measurements are given in Fig. 20.11. The thermocouples were positioned in the horizontal center of the cell. Five sensors were distributed vertically comprising the limits of the active cell area. Due to the influence of the external distributor manifold and the heat transfer in the upper bipolar plate region (sealing area) the minimum local temperature exceeds 120 °C at every position within the active cell area, although the cooling air enters the stack at ambient temperature. Towards the center of the cell the temperature rises linearly. Due to the missing insulation at the cooling air outlet at the bottom of the stack the temperature decreases slightly between the last two sensors. The maximum
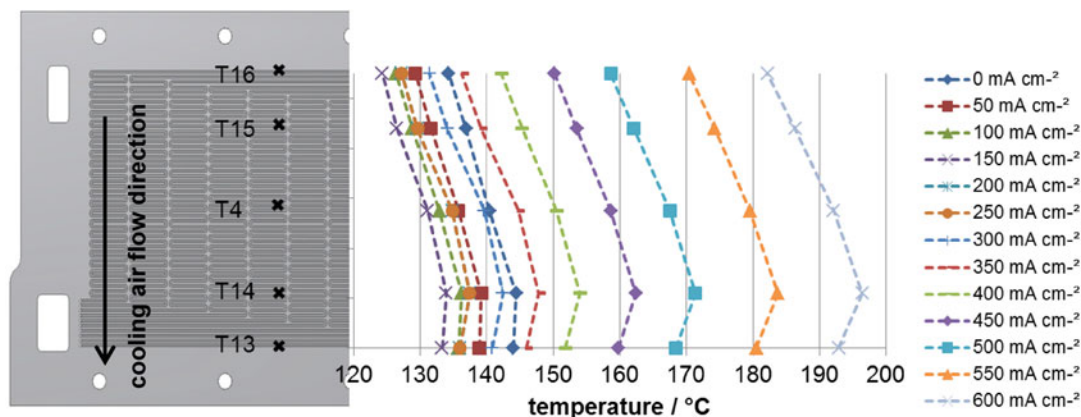
Fig. 20.11 Vertical temperature distribution across the active cell area for an air cooled stack where every cell is cooled

temperature gradient of 14.2 K was measured at a current density of 600 mA cm^{-2}. 180 °C as a limiting temperature was exceeded locally at a current density of 550 mA cm^{-2}.

One possibility to decrease the temperature gradients and the maximum local temperature is to increase and control the cooling air mass flow. As a drawback of this procedure the power consumption of the coolant blowers increases dramatically. For current densities of more than 800 mA cm^{-2} the blower consumed more than 14 % of the stack power [10].

In the next section we will present the test results with a liquid cooled stack setup. As another parameter the number of cooling cells in relation to the electrochemical cells (MEAs) was varied. The difference between the cooling of every cell and the cooling of every third cell are the omitted cooling structures, which leads to a stack size reduction. For the experiments the total mass flow of the coolant was set to a constant value of 4 kg min^{-1} at both configurations.

Regarding the temperature distribution between the single cells in a stack, cooling of each cell is advantageous but stack concepts where only every second or third cell is in contact with a cooling cell can also be found. For the chosen active cell area of 200 cm^2 a cooling of every third cell is possible [22]. However, this increases both the temperature gradient across the active cell area, as well as from cell to cell.

In order to demonstrate the differences between a cooling of each cell and a cooling of every third cell, two stacks based on the same concept (Fig. 20.10, right) have been build up to demonstrate experimentally the difference in the temperature profiles. The stack structure and the temperature measurement position for both stack concepts are shown in Fig. 20.12.

From Fig. 20.12 it can be seen that the temperature measuring positions are the same as for the tests with cooling air. Additionally the detailed sequence of the single components in the two setups is given. The results of the experimentally determined temperature distribution are shown in Fig. 20.13 for a stack where every cell is cooled and in Fig. 20.14 for a concept where every third cell is cooled.

Figures 20.13 and 20.14 indicate a rise in the average stack temperature level with rising current density due to the higher amount of heat to be dissipated in combination with the fixed cooling inlet conditions. Although the total volume flow rate of the cooling medium for both experiments is comparable the average temperature of the every-third-cell-cooled stack is 4 % higher. The reason is the increased distance between two cooling cells and the higher amount of heat to be dissipated by each cooling cell and thus the necessary temperature difference for the heat transfer.

For both cooling concepts it can be seen that the temperature first rises in flow direction with a
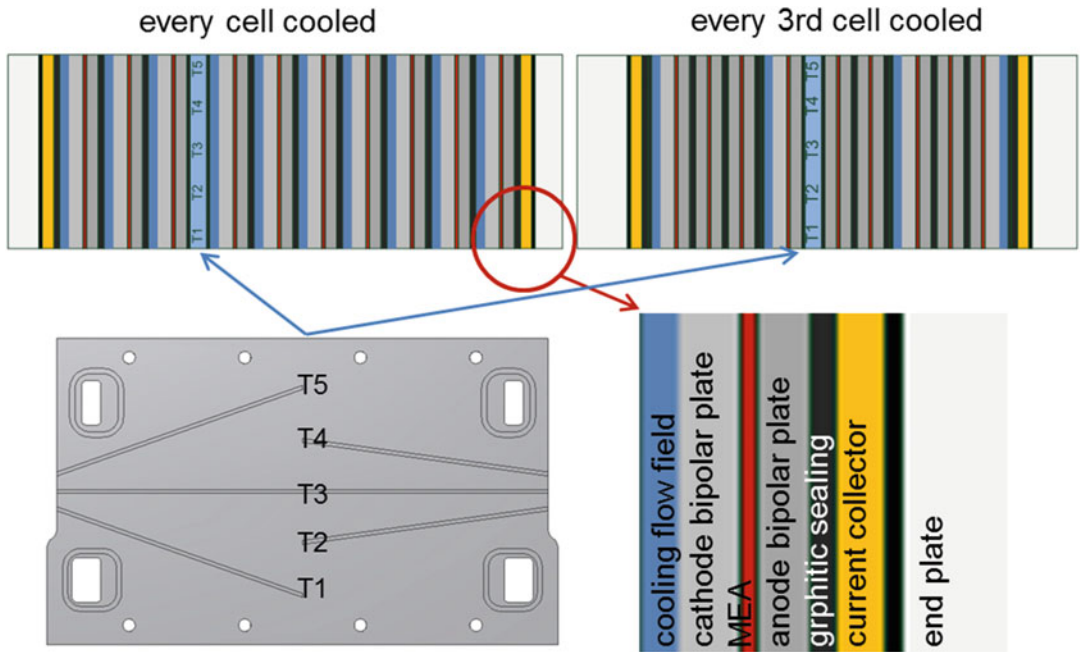
Fig. 20.12 Stack structure and temperature measurement positions
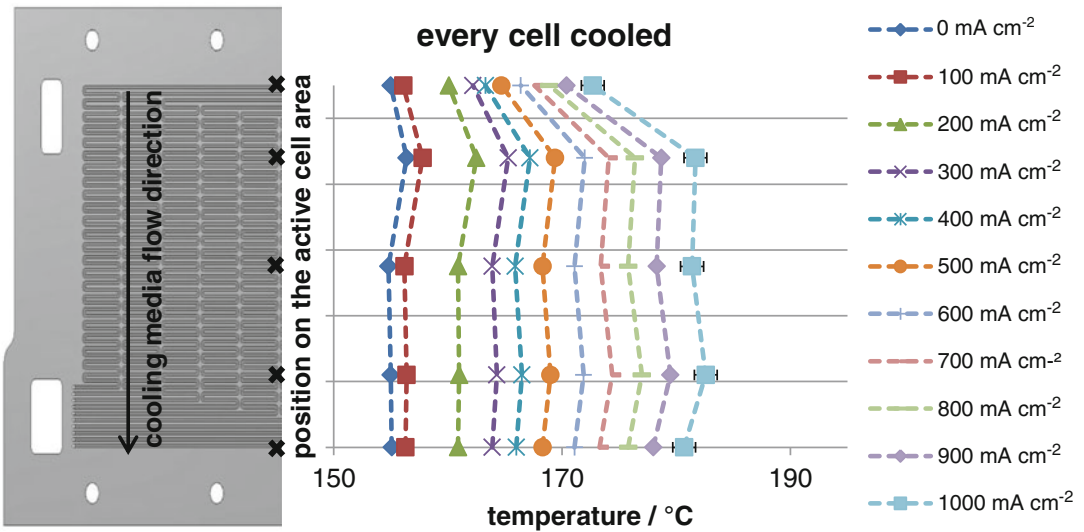

Fig. 20.13 Vertical temperature distribution across the active cell area for a stack where every cell is cooled

peak in the center of the stack and then falls slightly or remains at the same temperature level for higher current densities. The reason for this behavior is the temperature rise in the coolant due to the heat dissipation which is superimposed during the further progress of the heat dissipation by the non-ideal thermal insulation. In comparison to the every-cell-cooled concept the temperature difference for the every-third-cell cooled stack rises due to the higher amount of heat to be dissipated by each cooling cell. In average (over the whole operating range) the temperature
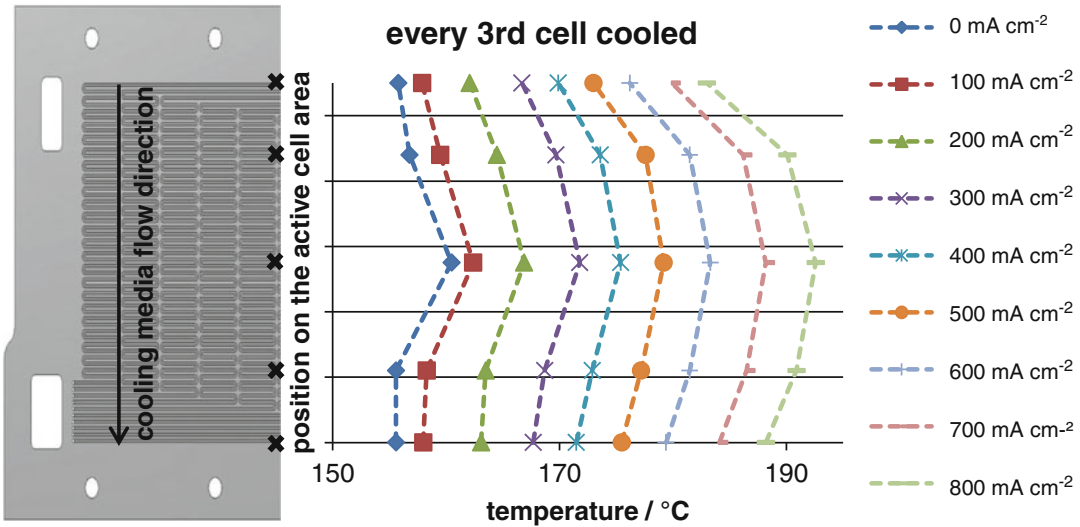
Fig. 20.14 Vertical temperature distribution across the active cell area for a stack where every third cell is cooled

difference is 35 % higher than for the stack were every cell is cooled. Nevertheless, the maximum temperature difference across the active cell area of less than 10 K occurring at the highest current density is relatively small for both stack concepts. The temperature difference from cell to cell for a stack where every third cell is cooled was published in [22]. It is clear that the maximum temperature was measured in the center cell between two cooling cells. For the allowed operation range, where the maximum local temperature does not exceed 180 °C, the maximum temperature difference is also in the range of 10 K. In general it can be stated that there is a clear relation between cell operation temperature and cell degradation rate. In [8] this was investigated systematically. So one can assume that the highest degradation rate will occur in the middle of the center cell at high current densities. The temperature difference as well as the maximum temperature can be limited by optimizing the cooling system in terms of coolant flow rate and coolant inlet temperature.

It can be concluded that both variants of cooling via forced convection in separate channels are well suited as an active thermal management concept for HT-PEMFC stacks. In the whole operating range the produced heat can be removed by means of this active cooling concept. Also heating up from ambient to operation temperature of the stack (>120 °C to avoid local condensation) is possible. On the systems level stack heating-up and cooling can be integrated into the thermal management of the reformer subsystem [23]. A start-up burner and an integrated cooling loop serve as main components of the thermal part of the system. As a consequence of this internal cooling concept the stack design has to provide for additional cooling structures which need to be integrated into the bipolar plate. This leads to further areas which need to be sealed and to an increase in the gravimetric and volumetric power density.

20.5 Alternative Cooling Concepts and Conclusions

Besides active cooling with air or with liquids like oil, stacks can also be cooled with water. The effects of water cooling are estimated by the authors only theoretically. The reason is the pressurization of the water cooling circuit, which is necessary not only for the conventional water cooling but also for the phase change concept. At ambient pressure of 1 bar the internal water cooling would cause a stack temperature of round about 100 °C due to the evaporation at
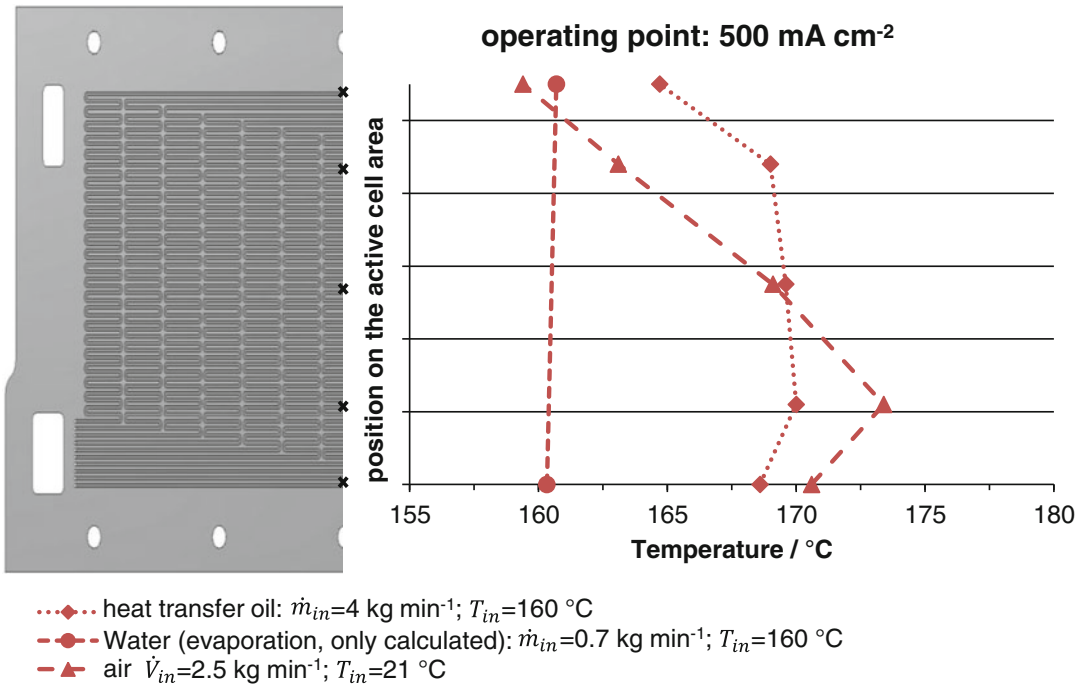
operating point: 500 mA cm⁻²

position on the active cell area

Temperature / °C

155   160   165   170   175   180

····◆··· heat transfer oil: $\dot{m}_{in}$=4 kg min⁻¹; T_{in}=160 °C
--●-- Water (evaporation, only calculated): $\dot{m}_{in}$=0.7 kg min⁻¹; T_{in}=160 °C
--▲-- air $\dot{V}_{in}$=2.5 kg min⁻¹; T_{in}=21 °C

Fig. 20.15 Comparison of the temperature distribution across the active cell area for three different cooling media at reformate operation

this temperature. Therefore a pressure of more than 5 bars is necessary to reach adequate operating temperatures. Due to this reason an experimental investigation of the temperature distribution for a water cooled stack was not performed with the described setup. Instead of this, calculations based on the energy balance equation were performed. The results of these calculations and the experimental investigations with thermo oil and air cooling are presented in Fig. 20.15 for a typical operating point at a current density of 500 mA cm⁻². From Fig. 20.15 it can be seen that all cooling concepts sufficiently cool the stack at this operating point. The lowest temperature gradient with 0.4 K across the active cell area can be achieved by water evaporation. The reason is the isothermal energy dissipation during the phase change. In comparison to water oil has a larger temperature gradient with 5.3 K across the active cell area. The largest temperature gradient of 14 K at this operating point was measured with air. The reason is the low specific heat capacity (1019 J kg⁻¹ K⁻¹ at 160 °C) and

the low heat transfer coefficient (<100 W cm⁻² K). Therefore a large volume flow or a high temperature gradient is required. The increase of the volume flow is limited by the heat transfer. This leads to the comparatively high temperature gradient.

Overall it can be concluded that oil, air, or water are suitable to cool HT-PEMFC stacks. Passive air cooling of a stack is not advisable because of the limited power range in an appropriate stack temperature range.

Active air cooling of stacks in the kW range is possible but a high energy demand for the external air blower limits the area of application. Another drawback of air cooling is that heating-up of the stack to the desired temperature typically requires an extra heating system. This can be implemented either by the introduction of an electric heating plate into the stack or by an additional electric air heater and heat exchanger.

Oil cooling has the advantages of effective heat removal at small temperature gradients, easy heat-up, robust behavior with a simplified

control of the heating system and good thermal integration into the entire system (fuel cell system and/or adjacent systems). Due to the high creeping capability of thermo oil the sealing of the cooling compartments inside the stack is a challenge. A leakage of oil with access to the gas compartment will cause MEA poisoning.

Cooling water has the highest potential due to the latent heat transfer but pressurization in the cooling loop is essential. Therefore heat transfer oil based cooling concepts are most practical.

References

1. Zhang J, Xie Z, Tang Y et al (2006) High temperature PEM fuel cells. J Power Sources 160:872–891
2. Lee SJ, Mukerjee S, Ticianelli EA et al (1999) Electrocatalysis of CO tolerance in hydrogen oxidation reaction in PEM fuel cells. Electrochim Acta 44:3283–3293
3. BASF (2012) Celtec® P1000 MEA. http://www.fuel-cell.basf.com/ca/internet/Fuel_Cell/en_GB/content/Microsite/Fuel_Cell/Products/Celtec-P_1000. Accessed 02 Aug 2012
4. Janßen H, Supra J, Lüke L et al (2013) Development of HT-PEFC stacks in the kW range. Int J Hydrog Energy 38:4705–4713
5. Serenergy (2014) S 165L—Liquid cooled HT PEM stack. http://serenergy.com/products/stacks/liquid-cooled-s165-l/. Accessed 21 Jul 2014
6. Lüke L, Janßen H, Kvesić M et al (2012) Performance analysis of HT-PEFC stacks. Int J Hydrog Energy 37:9171–9181
7. Pasel J, Meißner J, Porš Z et al (2007) Autothermal reforming of commercial Jet A-1 on a 5 kW$_e$ scale. Int J Hydrog Energy 32:4847–4858
8. Lüke L (2013) Analyse des Betriebsverhaltens von Hochtemperatur-Polymerelektrolyt-Brennstoffzellen, Schriften des Forschungszentrums Jülich, Reihe Energie & Umwelt/Energy & Environment Band/Volume 192. Dissertation, RWTH Aachen University. ISBN 978-3-89336-909-6
9. Verein Deutscher Ingenieure (Hrsg.) (2006) VDI-Wärmeatlas. 10. bearbeitete und erweiterte Auflage. Springer, Berlin
10. Supra J (2014) Kühlkonzepte für Hochtemperatur-Polymerelektrolyt-Brennstoffzellen-Stacks, Schriften des Forschungszentrums Jülich, Reihe Energie & Umwelt/Energy & Environment Band/Volume 209. Dissertation, RWTH Aachen University. ISBN 978-3-89336-946-1
11. Jensen H-C B, Kær SK (2011) Boundary model-based reference control of blower cooled high temperature polymer electrolyte membrane fuel cells. Int J Hydrog Energy 36:5030–5037
12. Kurz T, Keller J (2011) Heat management in a portable high temperature PEM fuel cell module with open cathode. Fuel Cells 11:518–525
13. Andreasen SJ, Ashworth L, Menjón Remón IN et al (2008) Directly connected series coupled HTPEM fuel cell stacks to a Li-ion battery DC bus for a fuel cell electrical vehicle. Int J Hydrog Energy 33:7137–7145
14. Andreasen SJ, Kær SK (2008) Modelling and evaluation of heating strategies for high temperature polymer electrolyte membrane fuel cell stacks. Int J Hydrog Energy 33:4655–4664
15. Andreasen SJ, Kær SK (2007) 400 W high temperature PEM fuel cell stack test. ECS Trans 5:197–207
16. Asghari S, Akhgar H, Imani BF (2011) Design of thermal management subsystem for a 5kW polymer electrolyte membrane fuel cell system. J Power Sources 196:3141–3148
17. Squadrito G, Giacoppo G, Barbera O et al (2010) Design and development of a 7kW polymer electrolyte membrane fuel cell stack for UPS application. Int J Hydrog Energy 35:9983–9989
18. Kvesic M (2012) Modellierung und Simulation von Hochtemperatur-Polymerelektrolyt-Brennstoffzellen, Schriften des Forschungszentrums Jülich, Reihe Energie & Umwelt/Energy & Environment Band/Volume 158. Dissertation, RWTH Aachen University. ISBN 978-3-89336-835-8
19. Bendzulla A (2010) Von der Komponente zum Stack: Entwicklung und Auslegung von HT-PEFC-Stacks der 5 kW-Klasse, Schriften des Forschungszentrums Jülich, Reihe Energie & Umwelt/Energy & Environment Band/Volume 69. Dissertation, RWTH Aachen University. ISBN 978-3-89336-634-7
20. Fragol (2014) FRAGOLTHERM® S-15-A. http://www.fragol.de/produkte/waermetraegerfluessigkeiten/produktuebersicht/fragolthermR-s-15-a.html. Accessed 6 June 2014
21. Eisenhuth (2013) SIGRACET bipolar plates BBP 4. http://www.eisenhuth.de/pages/frameset.html. Accessed 5 June 2013
22. Supra J, Janßen H, Lehnert W et al (2013) Temperature distribution in a liquid-cooled HT-PEFC stack. Int J Hydrog Energy 38:1943–1951
23. Samsun RC, Pasel J, Janßen H et al (2014) Design and test of a 5kW$_e$ high-temperature polymer electrolyte fuel cell system operated with diesel and kerosene. Appl Energy 114:238–249